



RESEARCH ARTICLE

Characterization and identification of elemental sulphur, iron pyrite, mineral gypsum, phospho gypsum and marine gypsum using SEM-EDAX

D Janaki^{1*}, P Gunavathi¹, P Balasubramaniam² & A Alagesan¹

¹Department of Soil Science and Agricultural Chemistry, Anbil Dharmalingam Agricultural College and Research Institute, Tiruchirappalli 620 009, Tamil Nadu, India

²Directorate of Natural Resource Management, Tamil Nadu Agricultural University, Coimbatore 641 003 Tamil Nadu, India

*Email: janaki.d@tnau.ac.in



ARTICLE HISTORY

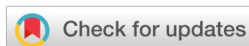
Received: 17 October 2024

Accepted: 06 January 2025

Available online

Version 1.0 : 26 January 2025

Version 2.0 : 28 January 2025



Additional information

Peer review: Publisher thanks Sectional Editor and the other anonymous reviewers for their contribution to the peer review of this work.

Reprints & permissions information is available at https://horizonpublishing.com/journals/index.php/PST/open_access_policy

Publisher's Note: Horizon e-Publishing Group remains neutral with regard to jurisdictional claims in published maps and institutional affiliations.

Indexing: Plant Science Today, published by Horizon e-Publishing Group, is covered by Scopus, Web of Science, BIOSIS Previews, Clarivate Analytics, NAAS, UGC Care, etc See https://horizonpublishing.com/journals/index.php/PST/indexing_abstracting

Copyright: © The Author(s). This is an open-access article distributed under the terms of the Creative Commons Attribution License, which permits unrestricted use, distribution and reproduction in any medium, provided the original author and source are credited (<https://creativecommons.org/licenses/by/4.0/>)

CITE THIS ARTICLE

Janaki D, Gunavathi P, Balasubramaniam P, Alagesan A. Characterization and identification of elemental sulphur, iron pyrite, mineral gypsum, phospho gypsum and marine gypsum using SEM-EDAX. Plant Science Today. 2025; 12(1): 1-8. <https://doi.org/10.14719/pst.5882>

Abstract

India has 6.73 million ha of salt-affected soils, of which 3.77 million ha is sodic soil. Sodicity is a serious issue in agriculture, and it prevents to meet the properties of fertile soil. Sodicity alters its physical and chemical properties, including soil structure and hydraulic conductivity. High exchangeable sodium and pH decrease soil permeability, available water capacity and infiltration rates through swelling and dispersion of clays as well as slaking of soil aggregates. Gypsum is one of the sources used for sodic soil reclamation, and the cheaper and alternative source is marine gypsum which is recovered from salt pans during production of common salt in coastal region, particularly in Gujarat and Tamil Nadu. The recovery of by-product gypsum and marine gypsum together is substantial and is comparable with the production of mineral gypsum. The amendments generally used for sodic soil reclamation should be a source of sulphates such as elemental sulphur, iron pyrite, mineral gypsum, phospho gypsum and marine gypsum. Characterization of sources by SEM-EDAX is rapid and elementary. The elemental composition revealed by the spectra of the bentonite sulphur for weight percentage and atomic percentage of sulphur is quantified as 34.04% and 18.59%, respectively, in the ZAF matrix. In iron pyrite spectra the weight percentage and atomic percentage of sulphur are 4.89% and 2.31%, respectively, in the ZAF matrix, while in mineral gypsum, the calcium weight percentage is 10.14% and atomic percentage is 04.04% while sulphur weight percentage is 6.52%, atomic percentage is 3.50%. The calcium composition in phosphogypsum is weight percentage is 14.69%; Atomic percentage is 34%, and the sulphur composition in phosphogypsum is weight percentage 10.40%, atomic percentage 5.60%, whereas in marine gypsum the calcium (weight percentage 09.10%, atomic percentage 03.58%) and sulphur (weight percentage 06.28%, atomic percentage 03.09%) proportions dominate as like two other above-mentioned gypsums, the element which makes difference in the marine gypsum from others is sodium (weight percentage 00.18%, atomic percentage 00.12%). This helps to confirm that marine gypsum is an economic and alternate source available for sodic soil reclamation.

Keywords

marine gypsum; mineral gypsum; phospho gypsum; SEM-EDAX; sulphur

Introduction

Gypsum is the main source used for sodic soil reclamation and it occurs in nature is called mineral gypsum. In addition to mineral gypsum, seawater and some chemical and fertilizer plants are sources of by-product of marine gypsum and chemical gypsum, respectively. The latter is obtained as by-product phosphogypsum or fluorogypsum or borogypsum, depending on the source. Phosphoric acid plants are important sources of by-product phosphogypsum. Marine gypsum is recovered from salt pans during the production of common salt in coastal regions, particularly in Gujarat and Tamil Nadu. The recovery of by-product gypsum and marine gypsum together is substantial and is comparable to the production of mineral gypsum. Synthetic gypsum is recovered via flue gas desulphurisation at some coal-fired electric power plants in Western countries (1).

Nature and cost of synthetic amendments recommended for sodic soil amelioration depend upon the soil properties, dosage, cost and capacity of sodium replacement. Among the various calcium sources, gypsum is most predominantly used as a reclaiming source of sodic soil, mainly due to low cost and efficiency. The low solubility and high requirement of water, decreases soil ESP. Hence, the quantity of amendment required is also reduced compared to other sources of reclamation (2).

The sources of amendments for sodic soil reclamation are currently scarce and costly. The characterization and analysis of such materials by chemical methods is tedious and destructive. The SEM-EDAX instrumental analysis is rapid, error-free and non-destructive. Even with micro-quantities of samples, it provides highly precise and reliable data. The elemental composition such as Ca, S, Na, Mg, Al, Si, P, Cl, K, Fe, Sr, Ba and Pb of gypsum was identified by using SEM and energy dispersive X-ray spectroscopy (1). The SEM – EDAX data will give precise results to study the composition of different sources due to the identification and analysis of multi-components as well as minor and traces in a systematic manner (3, 4). The objective of the study is to present and discuss the composition of different sources such as elemental sulphur, iron pyrite, mineral gypsum, phosphogypsum and marine gypsum. The majority of gypsum-specialist plants under study have crystals of both gypsum and calcium oxalate; however, other processes, such as the build-up of sulphates in organic molecules, are also consistent with plant specialization in gypsum (5). A broad range of iron sulfates has been described by their infrared and Raman fingerprints. Two coupled sodium/iron (III) sulfates, sideronatriite and ferrinatriite, received particular attention, and their infrared and Raman bands were partially assigned (6).

Marine gypsum is recovered from salt pans during the production of common salt in coastal regions, particularly in Gujarat and Tamil Nadu. The recovery of by-product gypsum and marine gypsum together is substantial and is comparable to the production of mineral gypsum. Synthetic gypsum is recovered *via* flue

gas desulphurisation at some coal-fired electric power plants in Western countries (7). These vibrations are modified when the sulfate anion is present within a solid-state medium, such as a mineral with a repeating molecular order, resulting in the potential appearance of sulfate vibration modes in the spectrum (8).

The relative abundance of aliphatic sulfur (thiol, thioether, and sulfone) in these coals decreased with increasing coal rank, according to the FTIR analysis of the organic sulfur structural parameters. In contrast, the relative abundance of aromatic sulfur in coal generally showed an increasing trend with increasing coalification (9). The experiment exhibits a negligible net effect ($\geq 0.03\%$ change) on the ratio of highly reactive iron phases (FeHR) to total iron (FeT), indicating that this redox proxy weathers rather conservatively. On the other hand, because of pyrite oxidation and iron (oxyhydr) oxide precipitation, weathering has a significant impact on the ratio of pyrite-bound iron to highly reactive iron (FePY/FeHR), which is used to examine the availability of sulfur (up to 32.5% difference) (10). There are various methods to characterise the elemental composition of sources of gypsum *viz.*, physio chemical analysis, and advanced instrumentation analysis using FTIR and SEM-EDAX. Laboratory analysis is exhaustive and time consuming, whereas instrumental analysis is easy and give precise and accurate results in shorter time. Hence in this study the elemental composition of different sources of gypsum is studied using scanning electron microscope – energy dispersive X-ray.

Materials and Methods

The amendments used for sodic soil reclamation such as elemental sulphur, iron pyrite, mineral gypsum, phosphogypsum and marine gypsum. The Quanta 250 model, SEM (Scanning Electron Microscope) is a type of microscope that uses Everhart-Thornley Detector as an electron detector. Tungsten is the source of electrons used. The FEI Quanta 250 FEG-SEM is equipped with a Schottky field emission gun and Everhart-Thornley detector for (secondary electrons) to deliver ultrahigh resolution (1.2 nm @ 30 kV), backscattered electron detector in high vacuum mode and large field secondary electron detector for low vacuum operation (3.0 nm @ 30 kV) imaging. The Quanta 250 successfully integrates with EDAX detectors that make it ideal for nanotechnology, materials science, biology, compositional and micro-structural imaging and analysis.

The Vacuum working distance is 3.99×10^{-4} Pascal. The powder sample was dispersed over a double-sided conductive carbon tape that had been fixed to the stub, and the ESEM (Environmental Scanning Electron Microscope) sample chamber was placed on top of the ESEM. After the filament was turned on and different parameters such as electron beam, intensity, spot size, accelerating voltage of 200 V-30 kV, operating voltage of 5-30 kV, magnification of 30X – 300 kX with a resolution of @ 30 kV (high vacuum conditions) of 1.2 nm @ 30 kV (low

vacuum conditions of 3.0 nm.

Energy Dispersive X-ray (EDAX) microanalysis is an elemental analysis technique based on the creation of distinctive X-rays that expose the existence of elements present in specimens. It is used in conjunction with electron microscopy. Both semi-qualitative and semi-quantitative information can be obtained from the EDAX microanalysis spectrum. EDAX is a useful tool for detecting nanoparticles. EDAX is also used to investigate contamination in the environment and to characterise mineral and element determination in samples.

Results and Discussions

Characterization of amendments using SEM-EDAX

Bentonite sulphur: The different magnifications of bentonite sulphur obtained from SEM *viz.* 50 μm , 30 μm , 10 μm and 5 μm are illustrated in Fig. 1-5. A porous texture is observed in SEM images of bentonite sulphur. The elemental composition is revealed by the spectra of bentonite sulphur in the (Fig. 5 and Table 1). The weight and atomic percentage of sulphur are quantified as 34.04% and 18.59% in the ZAF matrix respectively.

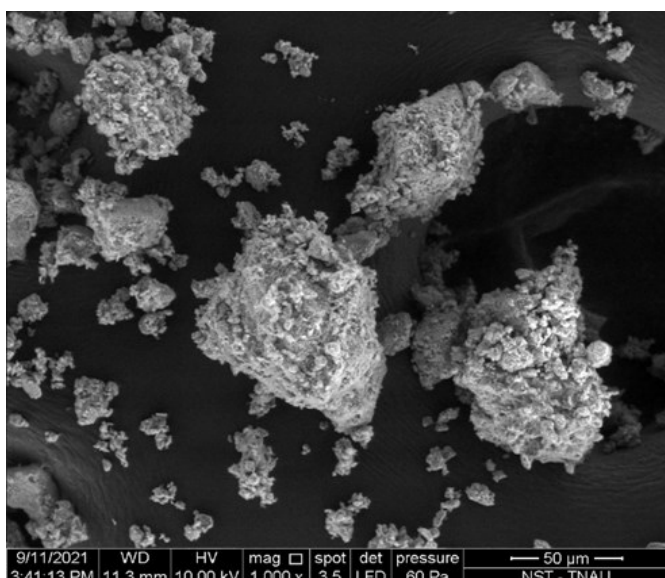


Fig. 1. SEM image of bentonite sulphur at 50 μm .

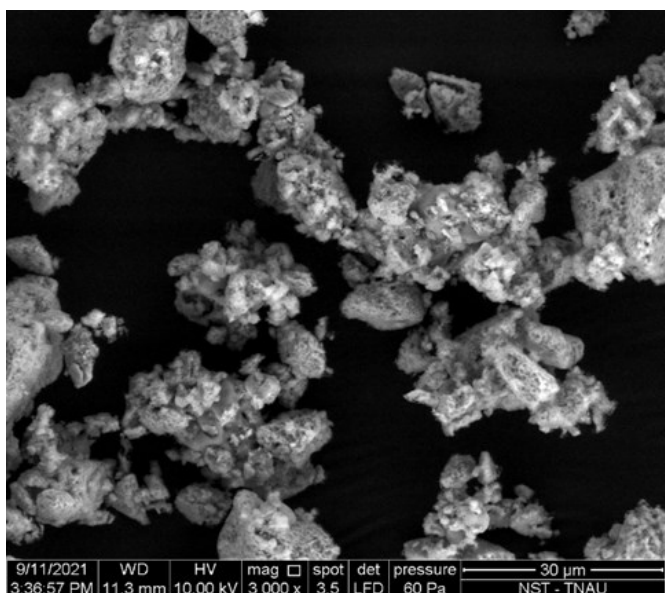


Fig. 2. SEM image of bentonite sulphur at 30 μm .

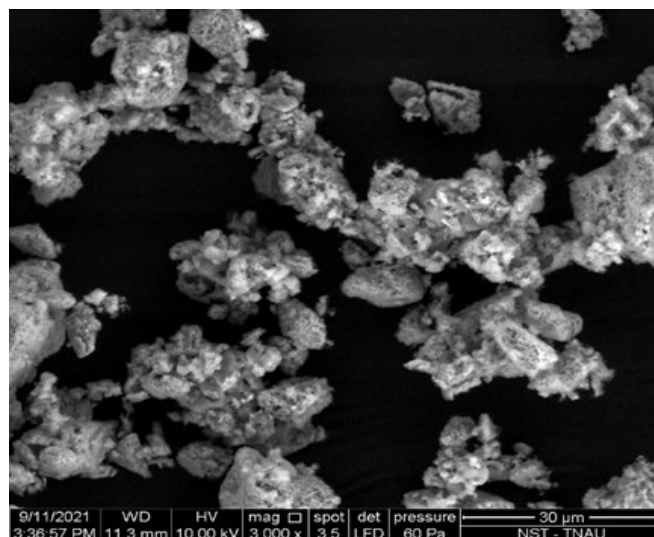


Fig. 3. SEM image of bentonite sulphur at 10 μm .

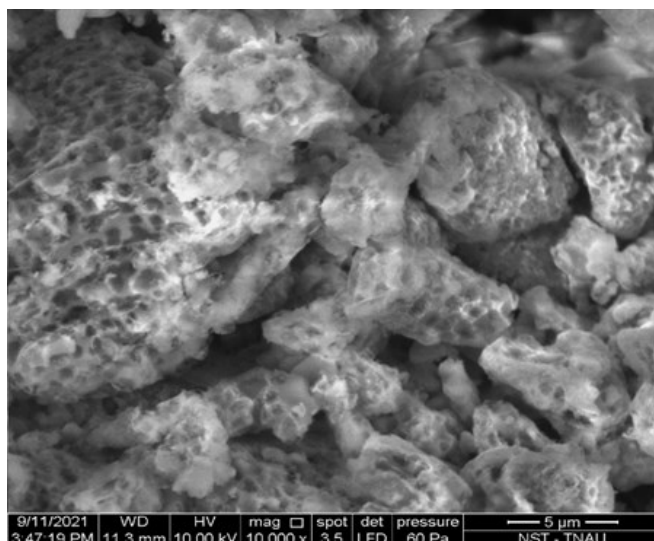


Fig. 4. SEM image of bentonite sulphur at 5 μm .

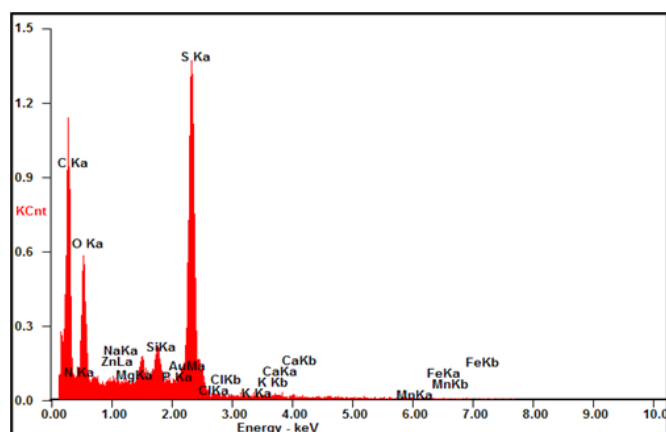


Fig. 5. Spectra of bentonite sulphur from EDAX.

Iron Pyrite: Fig. 6-10 depicts iron pyrite examined under a scanning electron microscope (SEM) at different magnifications of 50 μm , 30 μm , 10 μm and 5 μm . The well-defined images were observed in individual solid particles. The spectra and composition obtained from EDAX are shown in Fig. 10 and Table 1, respectively. The weight and atomic percentage of sulphur is quantified as 04.89% and 02.31%, in the ZAF matrix. The alcohol and hydroxyl compounds of dimeric, internally bonded, non-bonded, primary alcohol, secondary alcohol, tertiary alcohol and

Table 1. Composition of bentonite sulphur, iron pyrite, mineral gypsum, phospho gypsum and marine gypsum from SEM -EDAX

Sources	Bentonite Sulphur		Iron Pyrite		Mineral Gypsum		Phospho Gypsum		Marine Gypsum	
Element	WT %	AT %	WT %	AT %	WT %	AT %	WT %	AT %	WT %	AT %
CK	43.31	63.16	43.92	55.41	42.00	55.90	36.17	52.03	46.28	60.77
NK	03.22	04.03	12.68	13.72	11.51	13.14	00.54	00.67	02.71	03.05
OK	10.39	11.37	26.66	25.25	22.04	22.02	30.64	33.10	28.63	28.23
ZnL	00.00	00.00	00.00	00.00	00.27	00.07	00.67	00.18	00.00	00.00
NaK	00.20	00.15	00.00	00.00	00.00	00.00	00.00	00.00	00.18	00.12
MgK	00.05	00.03	00.00	00.00	00.21	00.14	00.15	00.11	00.42	00.27
SiK	02.02	01.26	01.05	00.57	00.78	00.44	01.34	00.83	00.76	00.43
PK	00.00	00.00	00.37	00.18	00.56	00.29	00.91	00.51	00.00	00.00
AuM	03.28	00.29	03.26	00.25	05.30	00.43	03.76	00.33	05.64	00.45
SK	34.04	18.59	04.89	02.31	06.52	03.25	10.40	05.60	06.28	03.09
ClK	00.00	00.00	00.00	00.00	00.19	00.09	00.00	00.00	00.00	00.00
KK	00.00	00.00	00.00	00.00	00.47	00.19	00.71	00.31	00.00	00.00
CaK	00.00	00.00	03.22	01.22	10.14	04.04	14.69	06.34	09.10	03.58
MnK	03.49	01.11	03.96	01.09	00.00	00.00	00.00	00.00	00.00	00.00
Matrix	Correction	ZAF	Correction	ZAF	Correction	ZAF	Correction	ZAF	Correction	ZAF

C - Carbon Mg - Magnesium Cl - Chloride
 N - Nitrogen Si - Silicon Cu - Copper
 O - Oxygen P - Phosphorus K - Potassium
 Zn - Zinc Au - Gold Ca - Calcium
 Na - Sodium S - Sulphur Mn - Manganese

WT%- Weight % AT%- Atomic % K, L, M- Electronic shell series ZAF- Atomic no, Absorption and fluorescent excitation

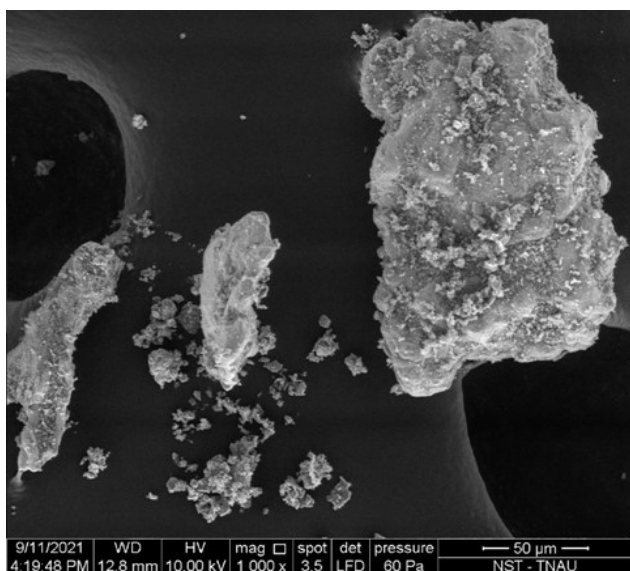


Fig. 6. SEM image of iron pyrite at 50 µm.

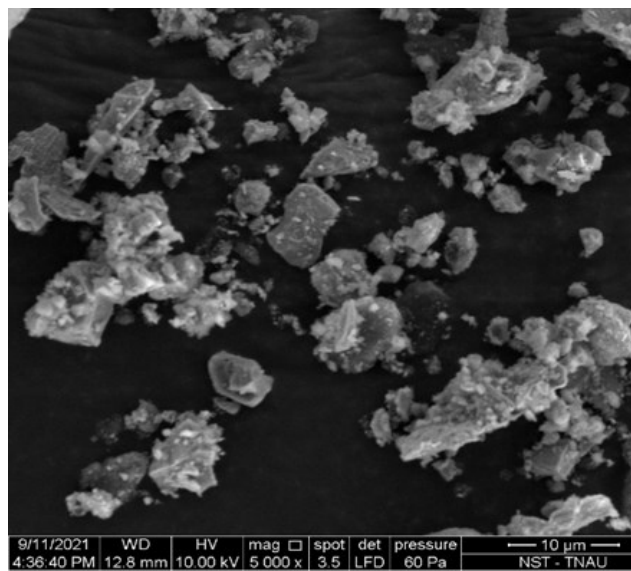


Fig. 8. SEM image of iron pyrite at 10 µm.

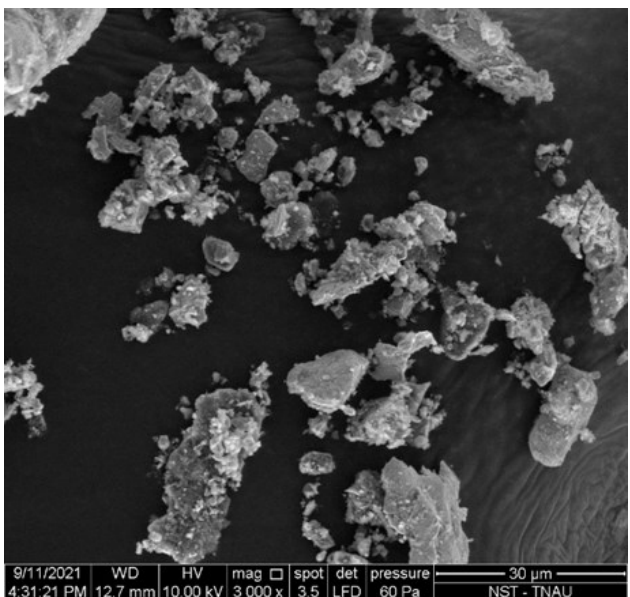


Fig. 7. SEM image of iron pyrite at 30 µm.

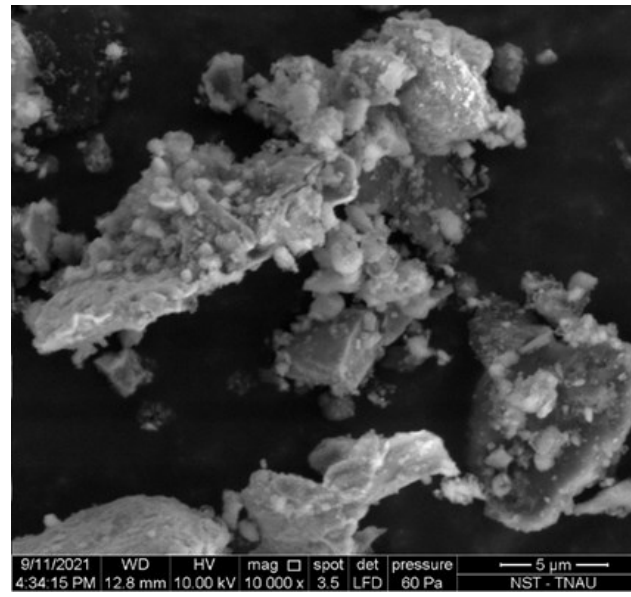


Fig. 9. SEM image of iron pyrite at 5 µm.

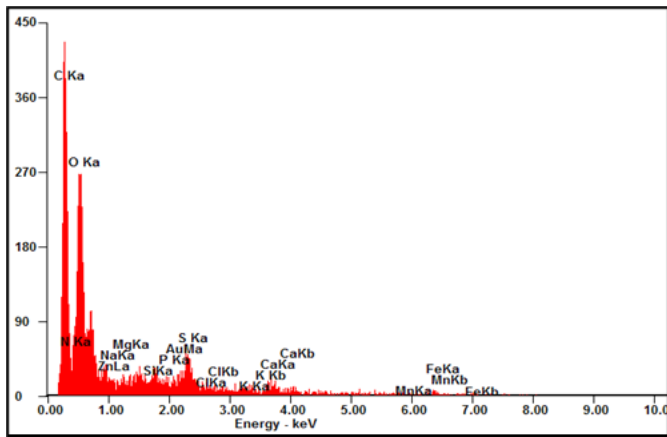


Fig. 10. Spectra of iron pyrite from EDAX.

phenols are observed in peaks of $3550\text{--}3450\text{ cm}^{-1}$, $3570\text{--}3540\text{ cm}^{-1}$, $3645\text{--}3600\text{ cm}^{-1}$, $3645\text{--}3630\text{ cm}^{-1}$, $3635\text{--}3620\text{ cm}^{-1}$, $3620\text{--}3540\text{ cm}^{-1}$ and $3640\text{--}3530\text{ cm}^{-1}$, respectively (11).

Mineral Gypsum: Fig. 11-15 reveals mineral gypsum investigated under a (SEM) at magnifications of $50\text{ }\mu\text{m}$, $30\text{ }\mu\text{m}$, $10\text{ }\mu\text{m}$ and $5\text{ }\mu\text{m}$. A flaky plate structure with uneven polished texture is observed in SEM image of mineral gypsum. Fig. 15 and Table 1 show the spectra and composition derived using EDAX. The elemental concentration of calcium (weight 10.14%, atomic 04.04%) and sulphur found to be highest followed by carbon, nitrogen and oxygen. The presence of a strong band centered around 1425.4 cm^{-1} , which are characteristics of the C–O stretching mode of carbonate together with a narrow band around 875.68 cm^{-1} of the bending mode of the carbonate of calcite. The calcium, sulphur and oxygen were high in elemental spectra of gypsum (2, 12, 13). The quantitative analysis model shows that the content was between 97.93% and 99.81% pure by specific method for identification of gypsum fibrosus by FTIR (14).

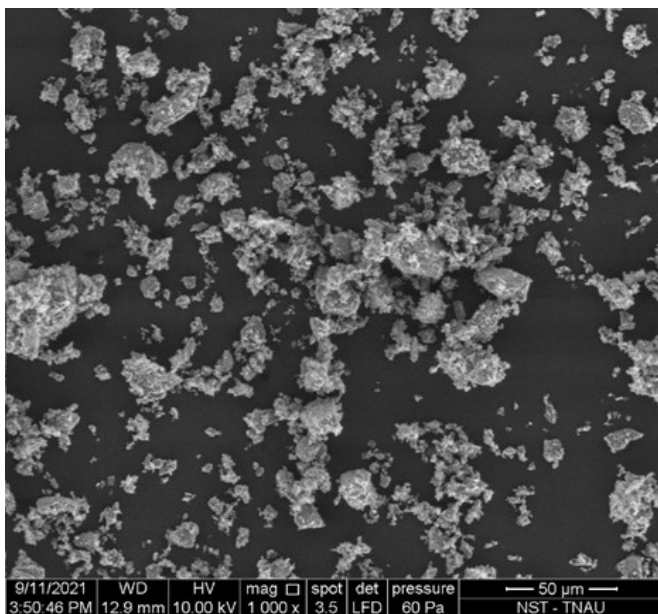


Fig. 11. SEM image of mineral gypsum at $50\text{ }\mu\text{m}$.

Phosphogypsum: The examination of phosphogypsum under SEM with various magnifications ($50\text{ }\mu\text{m}$, $30\text{ }\mu\text{m}$, $10\text{ }\mu\text{m}$ and $5\text{ }\mu\text{m}$) are given in Fig. 16-20. A uniformly smooth and silky texture is observed in the different

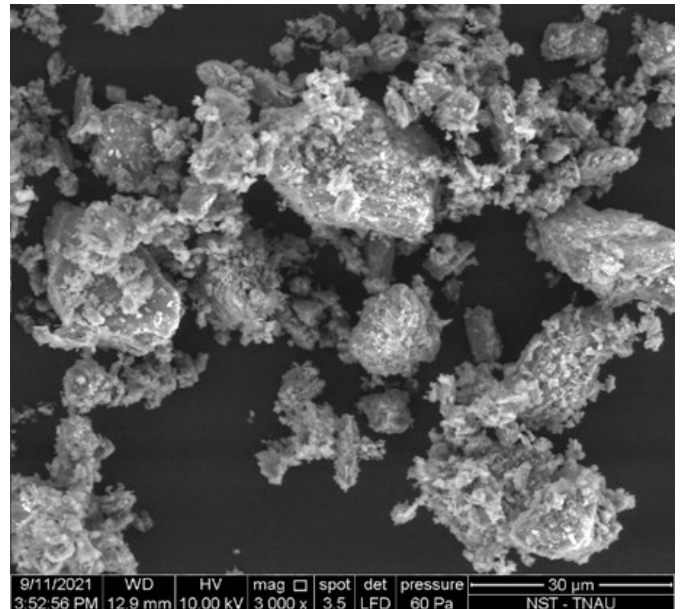


Fig. 12. SEM image of mineral gypsum at $30\text{ }\mu\text{m}$.

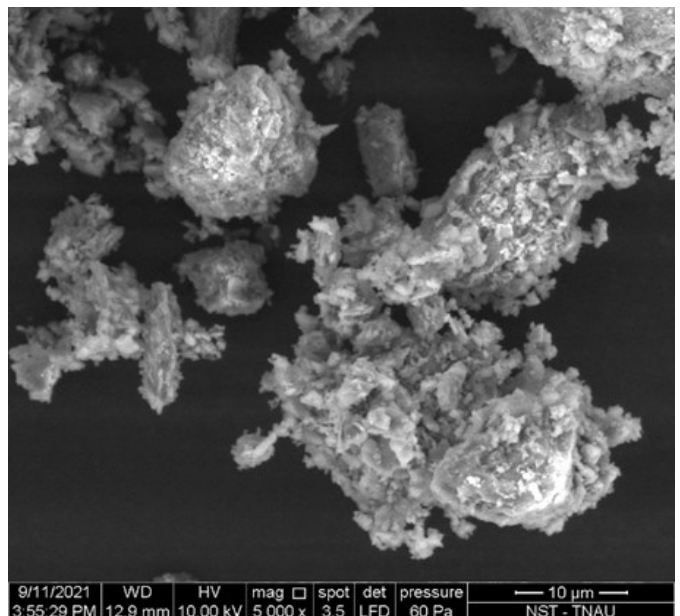


Fig. 13. SEM image of mineral gypsum at $10\text{ }\mu\text{m}$.

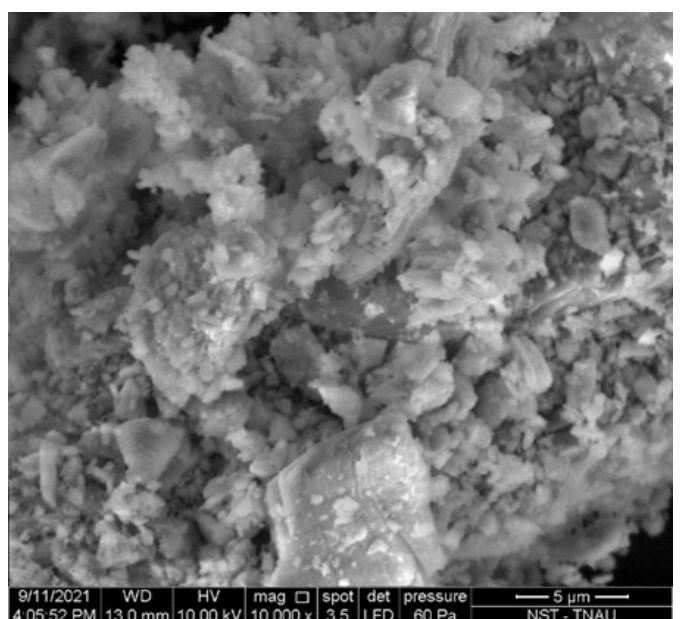


Fig. 14. SEM image of mineral gypsum at $5\text{ }\mu\text{m}$.

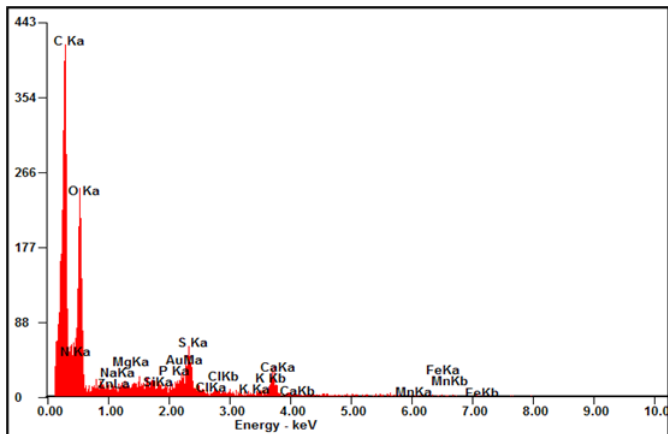


Fig. 15. Spectra of mineral gypsum from EDAX.

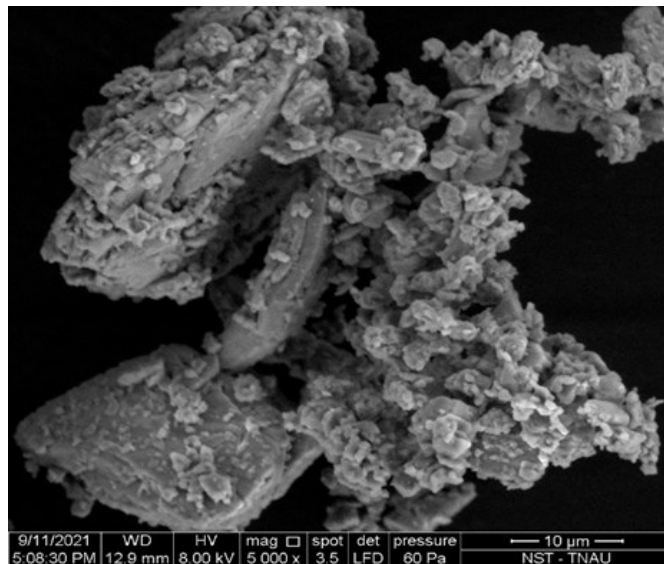


Fig. 18. SEM image of phospho gypsum at 10 μm.

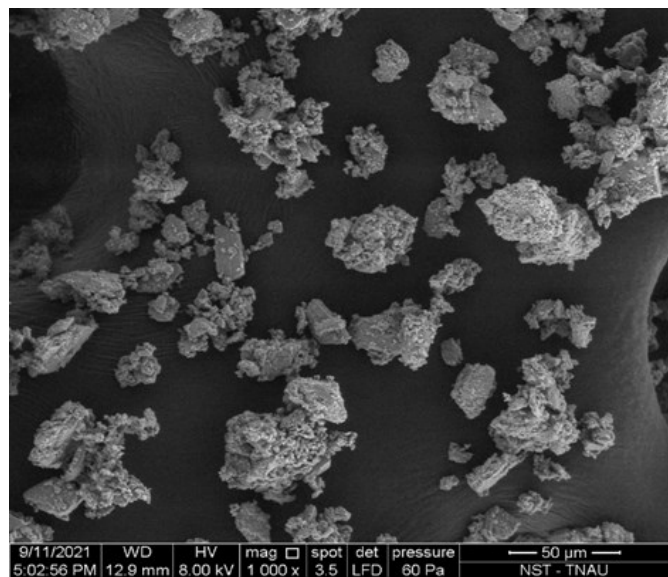


Fig. 16. SEM image of phospho gypsum at 50 μm.

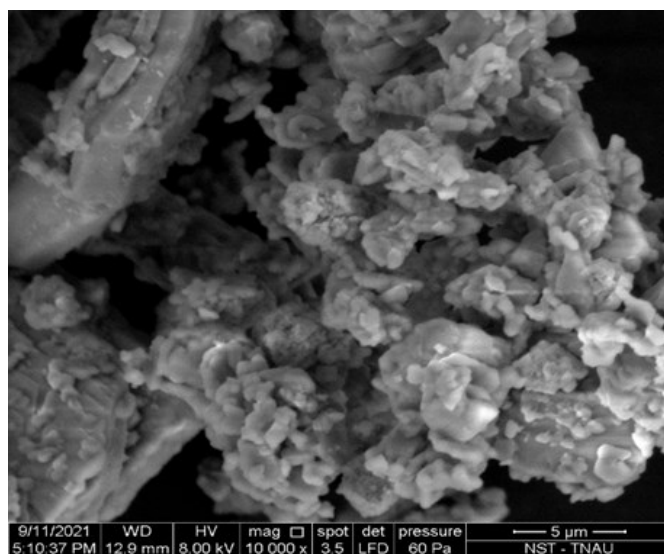


Fig. 19. SEM image of phospho gypsum at 5 μm.

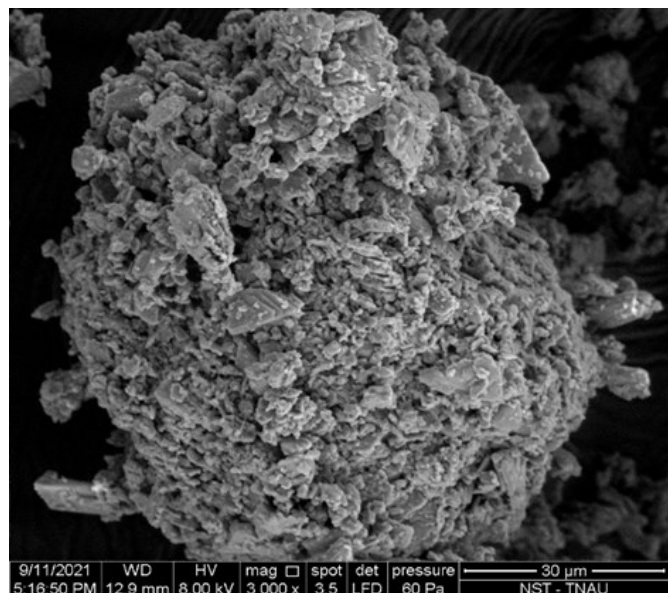


Fig. 17. SEM image of phospho gypsum at 30 μm.

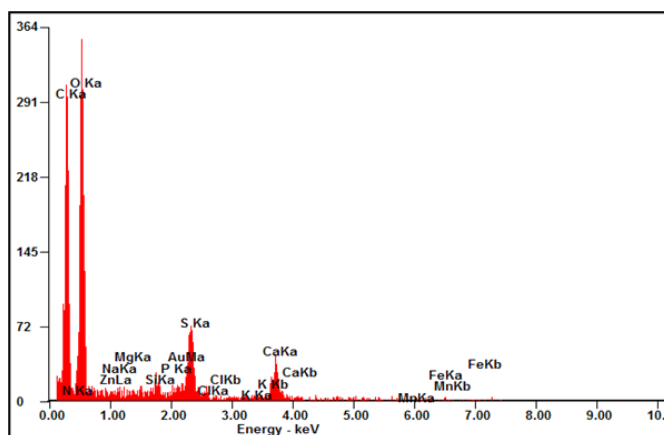


Fig. 20. Spectra of phospho gypsum from EDAX.

magnifications of phosphogypsum. The spectra of gypsum and their composition are shown in Fig. 20 and Table 1. As with mineral gypsum, weight percent of calcium 14.69%, atomic percent 06.34%, weight percent of sulphur 10.40%, atomic percent 05.60% obtained higher after the carbon, nitrogen and oxygen in ZAF matrix. This is in line with (1, 11). Gypsum and bassanite spectra exhibit characteristic and distinct triplet bands near 1.4-1.5 μm, a strong band

near 1.93-1.94 μm, and multiple features near 2.1-2.3 μm attributed to H₂O. Anhydrite, bassanite, and gypsum all have SO₄ combination and overtone features from 4.2-5 μm that are present in reflectance spectra (15). The sulphate concentration of mineral gypsum. It varied from 2.54 meq l⁻¹ to 3.49 meq l⁻¹ which has been extensively studied in recent years (16).

Marine gypsum: Marine gypsum examined under SEM by different magnifications of 50 μm , 30 μm , 10 μm and 5 μm are represented in the Fig. 21-25, respectively. An angular thylakoid like arrangement is identified in SEM image of marine gypsum and the spectra and composition obtained from EDAX, it is given in the Fig. 25 and Table 1 respectively. The calcium (weight 09.10%, atomic 03.58%) and sulphur (weight 06.28%, atomic 03.09%) proportions dominate as like two other above-mentioned gypsums, the element which makes difference in the marine gypsum from others is sodium (weight 00.18%, atomic 00.12%) that also quantified well. Sulfate mode frequencies such as ν_1 , ν_2 , ν_3 , and ν_4 are similar for all Ca-sulfates spectra. A broad peak is observed in ν_2 vibration for gypsum (9). The present findings are in consonance with (2, 12). It is also reported that gypsum fibrosum was investigated by infrared spectrum coupled with inductively coupled plasma mass spectrometry (ICP-MS), which is related to the content of elements, such as Ca, Mg, Zn and Na (17).

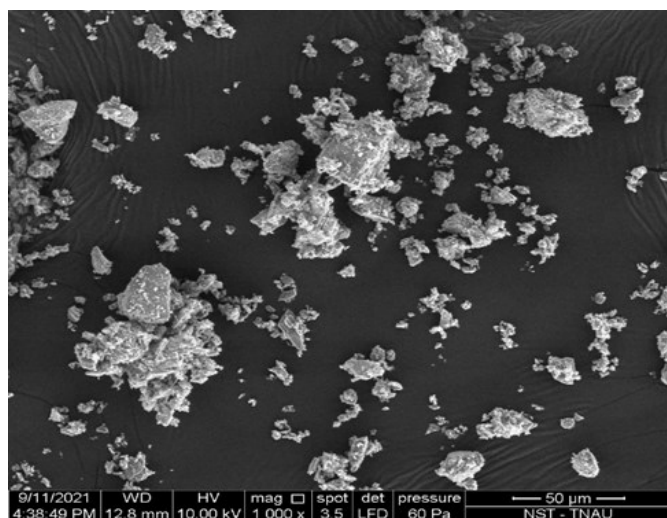


Fig. 21. SEM image of marine gypsum at 50 μm .

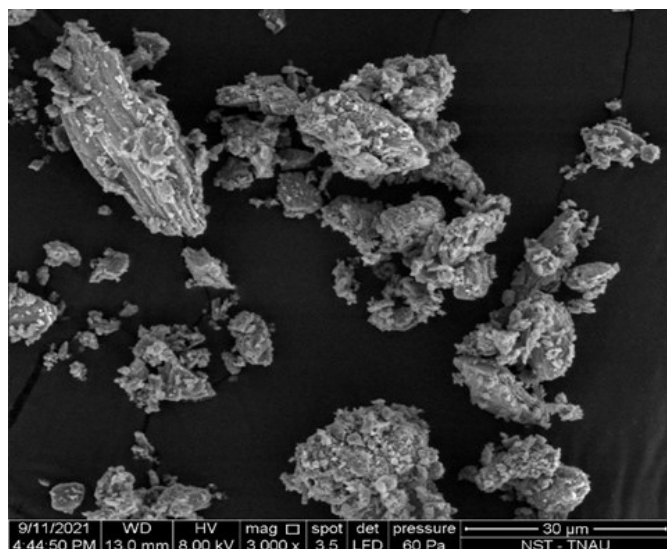


Fig. 22. SEM image of marine gypsum at 30 μm .

Conclusion

The ZAF matrix quantifies the weight percentage and atomic percentage of sulphur as 34.04% and 18.59%,

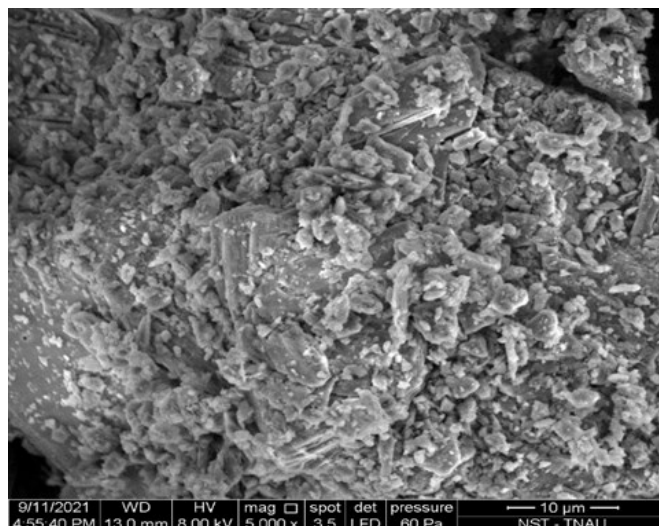


Fig. 23. SEM image of marine gypsum at 10 μm .

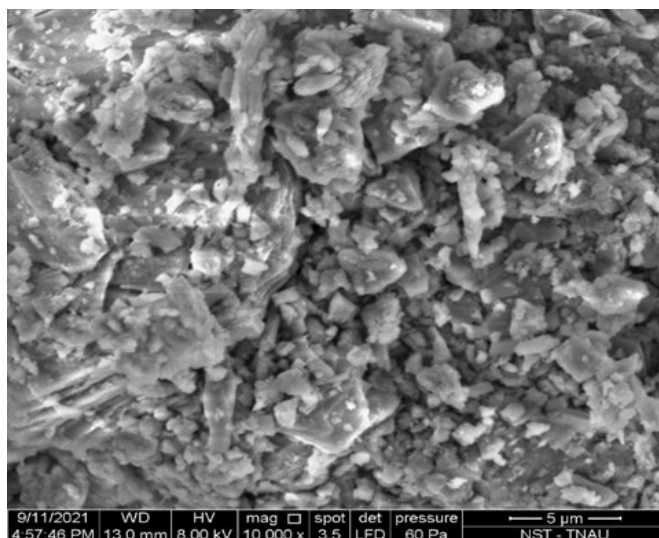


Fig. 24. SEM image of marine gypsum at 5 μm .

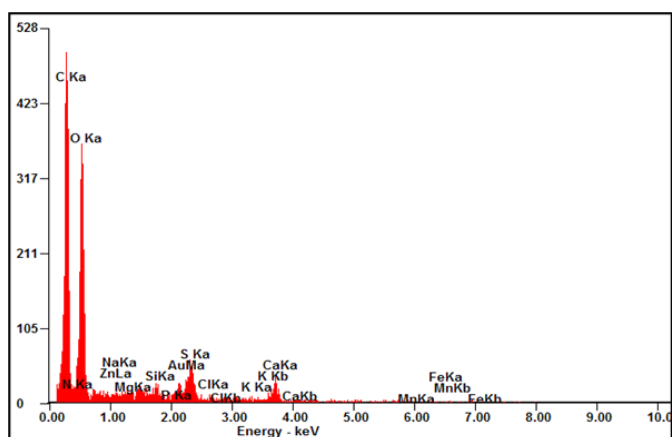


Fig. 25. Spectra of marine gypsum from EDAX.

respectively, revealing the components' composition. In the ZAF matrix, the weight percentage and atomic percentage of sulfur in iron pyrite are 4.89% and 2.31%, respectively, but in natural gypsum, calcium weight percentage is 10.14% and atomic percentage is 04.04% and sulfur is 6.52% and 3.50%. In phosphogypsum, the calcium composition is (weight 14.69%, and 6.34%) and the sulfur composition is (weight 10.40%, 5.60%). In contrast, in marine gypsum, the proportions of calcium (weight 09.10%, 03.58%) and sulphur (weight 06.28%, 03.09%) predominate, just like in the other two gypsums

mentioned above. The element that distinguishes marine gypsum from the others is sodium (weight 00.18% and atomic 00.12%) as the source is from sea and the results confirm that same can be used as alternate a cheap source for sodic soil reclamation

Acknowledgements

The authors wishes to thank Department of Nano science and Technology, Tamil Nadu Agricultural University, Coimbatore for providing necessary support and facilities to take SEM analysis.

Authors' Contributions

PG conducted the experiment and drafted the manuscript. DJ contributed to the supervision of research project and data analysis and edited the manuscript PB helped in editing the manuscript and provided valuable insights. AA helped in taking the reading in SEM analysis. All authors have read and approved the final manuscript.

Compliance with Ethical Standards

Conflict of interest: Authors do not have any conflict of interests to declare.

Ethical issues: None

Declaration of generative AI and AI-assisted technologies in the writing process

Grammarly AI tool was used to improve language and readability, with caution. After using this tool, the authors reviewed and edited the content as needed and takes full responsibility for the content of the publication.

References

- MINES IBO. Indian Minerals Yearbook 2016: Government of India, Ministry of Mines, Nagpur; 2016
- Prather R, Goertzen J, Rhoades J, Frenkel H. Efficient amendment use in sodic soil reclamation. *Soil Sci Soc Am J.* 1978;42(5):782–86. <https://doi.org/10.2136/sssaj1978.03615995004200050027x>
- Antunes V, Candeias A, Oliveira MJ, Longelin S, Serrão V, Seruya AI, et al. Characterization of gypsum and anhydrite ground layers in 15th and 16th centuries Portuguese paintings by Raman Spectroscopy and other techniques. *J Raman Spectrosc.* 2014;45(11-12):1026–33. <https://dx.doi.org/10.1002/jrs.4488>
- La Russa MF, Ruffolo SA, Barone G, Crisci GM, Mazzoleni P, Pezzino A. The use of FTIR and micro-FTIR spectroscopy: An example of application to cultural heritage. *Int J Spectrosc.* 2009;2009:893528. <https://doi:10.1155/2009/893528>
- Wei Y, Jun-Cheng L, Shu-Mei W, Sheng-Wang L, Jiang-Yong Y. The FTIR fingerprint of gypsum fibrosum. *Acta Medica Mediter.* 2016;32:607–11. [https://doi.org/10.3964/j.issn.1000-0593\(2016\)07-2098-06](https://doi.org/10.3964/j.issn.1000-0593(2016)07-2098-06)
- Palacio S, Aitkenhead M, Escudero A, Montserrat-Martí G, Maestro M, Robertson AJ. Gypsophile chemistry unveiled: Fourier transform infrared (FTIR) spectroscopy provides new insight into plant adaptations to gypsum soils. *PLoS One.* 2014;9(9):107285. <https://doi.org/10.1371/journal.pone.0107285>
- Rouchon V, Badet H, Belhadj O, Bonnerot O, Lavédrine B, Michard JG, et al. Raman and FTIR spectroscopy applied to the conservation report of paleontological collections: Identification of Raman and FTIR signatures of several iron sulfate species such as ferrinatrite and sideronatrite. *J Raman Spectrosc.* 2012;43(9):1265–74. <https://doi.org/10.1002/jrs.4041>
- Lane MD. Mid-infrared emission spectroscopy of sulfate and sulfate-bearing minerals. *Am Mineralog.* 2007;92(1):1–18. <https://doi.org/10.2138/am.2007.2170>
- Tang Y, Chen C, Li X, Wei Q, Guo X, Finkelman RB, et al. The evolution characteristics of organic sulfur structure in various Chinese high organic sulfur coals. *Energy Explor Exploit.* 2021;39(1):336–53. <https://doi.org/10.1177/0144598720975142>
- Mahoney C, Marz C, Buckman J, Wagner T, Vladmir Orlando V. Pyrite oxidation in shales: Implication for paleo-redox proxies based on geochemical and SEM-EDX evidence. *Sedim Geol.* 2019;289:186–98. DOI: 10.1016/j.sedgeo.2019.06.006
- Coates J. Interpretation of infrared spectra, a practical approach. *Encyclopedia of analytical chemistry.* J Wiley and Sons Ltd. Chichester. 2000; p.10815–37. <https://doi.org/10.1002/9780470027318.a5606>
- Adekola FA, Olosho AI, Baba AA, Adebayo SA. Dissolution kinetics studies of Nigerian gypsum ore in hydrochloric acid. *J Chem Tech Metal.* 2018;53(5):845–55.
- Al Dabbas M, Eisa MY, Kadhim WH. Estimation of gypsum-calcite percentages using a Fourier transform infrared spectrophotometer (FTIR), in Alexandria Gypsiferous Soil-Iraq. *Iraqi J Sci.* 2014;55(4b):1916–26. <https://www.ijs.uobaghdad.edu.iq/index.php/eijs/article/view/10812>
- Yuan M, Sun X, Chen L, Zhang Y, Fan Y. Rapid determination of CaSO₄·2H₂O in gypsum by Raman spectra. *Chinese Pharma.* 2015;18:73–76. <https://doi.org/10.1021/ac501932f>
- Bishop JL, Lane MD, Dyar MD, King SJ, Brown AJ, Swayze GA. Spectral properties of Ca-sulfates: Gypsum, bassanite and anhydrite. *Am Mineral.* 2014;99(10):2105–15. <https://doi.org/10.2138/am-2014-4756>
- Klimchouk A. The dissolution and conversion of gypsum and anhydrite. *Int J Spel.* 1996;25(3):2. <http://dx.doi.org/10.5038/1827-806X.25.3.2>
- Bao Y, Yang X, Wang S, Bian J, Yu Y. Difference of material base of gypsum before and after processing drugs by IR spectroscopy and ICP-MS. *Chinese J Spectrosc Lab.* 2012;29:3293–97.